doi.org/10.36721/PJPS.2026.39.12.345.1

Site-specific transdermal delivery of Qingteng Waifu San in a rheumatoid arthritis rabbit model

Yuan Gao[1], Lei Chi[2], Kun Gao[1], Yanning Liu[1] and Mengdan Zhou[3]*

[1]College of Pharmacy, Guizhou University of Traditional Chinese Medicine, Guiyang 550025, Guizhou, China
[2]Department of Acupuncture and Moxibustion, The Second Affiliated Hospital of Heilongjiang University of Chinese Medicine, Harbin 150000, Heilongjiang, China
[3]Department of Acupuncture and Moxibustion, Affiliated Hospital of Guizhou Medical University, Guiyang 550001, Guizhou, China

Abstract: **Background**: Rheumatoid arthritis (RA) is a chronic autoimmune disease characterized by synovial inflammation, joint swelling, pain, cartilage destruction and bone erosion. Qingteng Waifu San is an external sinomenine-containing preparation, but its site-specific transdermal response requires disease-relevant evaluation. **Objectives**: To compare Zusanli (ST36)-site and adjacent non-acupoint transdermal application of Qingteng Waifu San in an ovalbumin/complete Freund's adjuvant-induced RA rabbit model and to evaluate formulation, neuropeptide, inflammatory, behavioural and histopathological outcomes. **Methods**: Forty-eight New Zealand white rabbits were allocated into six groups (n=8 each): normal control, vehicle-only transdermal control, acupuncture, acupoint injection, ST36-site transdermal Qingteng Waifu San and adjacent non-acupoint transdermal Qingteng Waifu San. Gel appearance, pH, viscosity, spreadability, sinomenine content and high-performance liquid chromatography (HPLC) fingerprint similarity were assessed. Substance P (SP), calcitonin gene-related peptide (CGRP), tumor necrosis factor-alpha (TNF-alpha), interleukin-6 (IL-6) and interleukin-1 beta (IL-1beta) were measured by enzyme-linked immunosorbent assay (ELISA). SP and CGRP messenger RNA (mRNA) were analysed by real-time polymerase chain reaction (PCR). Arthritis score, paw volume, mechanical withdrawal threshold and histopathological scores were assessed. **Results**: The vehicle-only group showed RA-related changes compared with normal controls. ST36-site Qingteng Waifu San reduced arthritis score, paw volume, serum cytokines and histopathological injury scores and improved mechanical withdrawal threshold compared with vehicle-only control. SP and CGRP levels were higher after ST36 application than after adjacent non-acupoint application, indicating site-dependent neurocutaneous modulation. **Conclusion**: ST36-site transdermal Qingteng Waifu San produced stronger neuropeptide modulation and more favourable RA-related outcome profiles than adjacent non-acupoint application.

Keywords: Calcitonin gene-related peptide; Inflammatory cytokines; Qingteng Waifu San; Rheumatoid arthritis; ST36; Substance P; Transdermal delivery

Submitted on 09-05-2026 – Revised on 05-08-2026 – Accepted on 16-08-2026 – Available online on 27-08-2026 – Published on 01-12-2026

INTRODUCTION

Rheumatoid arthritis (RA) is a chronic autoimmune inflammatory disease characterized by persistent synovitis, pain, cartilage degradation and bone erosion. Current pharmacological treatment can relieve symptoms, but incomplete response, adverse reactions and poor tolerance remain important clinical challenges (Xu *et al*., 2023; Wang *et al*., 2025). Therefore, adjunctive local therapies with reduced systemic exposure remain of interest.

Transdermal drug delivery has advantages including avoidance of first-pass metabolism, local exposure, sustained release and improved convenience. Recent studies have explored transdermal, vesicular, microneedle and acupoint-associated delivery systems for RA, including sinomenine-loaded transethosomes, triptolide microneedles and sinomenine-based topical strategies (Song *et al*., 2019; Wang *et al*., 2019). In the present study, the traditional acupoint-application model was described as a site-specific transdermal drug delivery system, focusing on whether the local skin site, microcirculation and sensory neurovascular distribution influence pharmacological responses.

Qingteng Waifu San was defined in this study as a sinomenine-containing external preparation. The principal active ingredient was sinomenine, derived from Sinomenium acutum, and dispersed in a hydrophilic gel vehicle for topical application. Sinomenine and related formulations have been reported to regulate inflammatory cytokines, immune cell responses, matrix metalloproteinase-9-related inflammation, interleukin-6-related mechanisms and

**Corresponding author:* e-mail: z13985054992@126.com

Table 1: Apparatus, reagents and their use in the study.

Instrument/Reagent	Manufacturer or source	Use in study
AB265-S electronic analytical balance	Torontech Group International Inc., China	Weighing reagents and drug material
NanoDrop 2000 spectrophotometer	Thermo Fisher Scientific, China	RNA concentration and purity assessment
DF-101Z magnetic stirrer	Greatwall Scientific Industrial and Trade Co., Ltd., China	Preparation of topical gel/solution
5423 R refrigerated centrifuge	Eppendorf AG, Germany	Serum/tissue homogenate centrifugation
Mini-Beadbeater-16 tissue homogenizer	BioSpec Products Inc., USA	Tissue homogenisation
Microplate reader (ELx800, 450 nm)	BioTek Instruments, Inc., USA	ELISA absorbance measurement
ABI 7500 Real-Time PCR System	Applied Biosystems, USA	Real-time PCR amplification
Rabbit SP ELISA kits	Summus Biotechnology Co., Ltd., China	Measurement of SP in serum and tissue
Rabbit CGRP ELISA kits	Summus Biotechnology Co., Ltd., China	Measurement of CGRP in serum and tissue
Rabbit TNF-alpha, IL-6 and IL-1beta ELISA kits	Summus Biotechnology Co., Ltd., China	Measurement of inflammatory cytokines
Ovalbumin (OVA, A5253)	Sigma-Aldrich, USA	RA model induction
Complete Freund's adjuvant (CFA, F5881)	Sigma-Aldrich, USA	RA model induction
Qingteng Waifu San/sinomenine raw material	Chengdu Must Bio-Technology Co., Ltd., China	Topical and injection intervention
HPLC system for chemical fingerprinting	Agilent Technologies, USA	Quality-control fingerprinting of Qingteng Waifu San
Sinomenine reference standard	Chengdu Must Bio-Technology Co., Ltd., China	Identification of the main active component in chemical fingerprinting

joint inflammation in RA-related studies (Zhang *et al*., 2022; Liu *et al*., 2024). However, the local neuropeptide response and the site-specific transdermal effects of Qingteng Waifu San remain incompletely elucidated.

Substance P (SP) and calcitonin gene-related peptide (CGRP) are neuropeptides involved in neurogenic inflammation, vasodilation and pain signaling. Their elevation should not be assumed to confer therapeutic benefit on its own, particularly in RA (Green, 2005; Lisowska *et al*., 2015; Walsh *et al*., 2015).

Therefore, the study combined SP/CGRP assessment with RA-related outcome indicators including joint swelling, paw volume, pain behavior, inflammatory cytokines and histopathology. The objective was to compare Zusanli (ST36)-site and adjacent non-acupoint transdermal delivery of Qingteng Waifu San and to clarify whether site-specific neurocutaneous responses are associated with disease-relevant RA outcomes.

MATERIALS AND METHODS

Apparatus, reagents and formulation

The main apparatus and reagents for ribonucleic acid (RNA), enzyme-linked immunosorbent assay (ELISA), polymerase chain reaction (PCR), high-performance liquid chromatography (HPLC), tumor necrosis factor-alpha (TNF-alpha), interleukin-6 (IL-6) and interleukin-1 beta (IL-1beta) analyses are listed in table 1. The Qingteng Waifu San preparation intended for transdermal application was a hydrophilic gel containing sinomenine. The active raw material was sinomenine, with a purity of not less than 98% (Chengdu Must Bio-Technology Co., Ltd., China). The vehicle base contained a hydrophilic gel matrix and water for injection.

Preparation and characterization of topical gel and injection solution

The topical Qingteng Waifu San gel was prepared as a sinomenine-containing hydrophilic semisolid formulation. Briefly, Carbomer 940 was slowly dispersed in water for injection under magnetic stirring and allowed to fully hydrate. Sinomenine raw material was accurately weighed according to the target dose, dissolved or uniformly dispersed in the aqueous phase and then incorporated into the pre-hydrated gel matrix. Glycerol was added as a humectant and consistency modifier and triethanolamine was added dropwise to neutralize the Carbomer dispersion until a

homogeneous gel was obtained. The vehicle-only gel was prepared using the same procedure without sinomenine. The prepared gel was equilibrated for 24 h at 4°C and returned to room temperature before use. The acupoint injection solution was freshly prepared by dissolving sinomenine in sterile water for injection at the specified dose, then filtered through a 0.22 μm sterile membrane and visually inspected for clarity before administration (Jin *et al*., 2022).

Formulation characterization was performed to support reproducibility of local transdermal delivery. The gel and injection solution were evaluated for appearance, homogeneity, pH, viscosity, spreadability, drug content and chemical fingerprinting. pH was measured using a calibrated PHS-3C pH meter, viscosity was measured at 25°C using an NDJ-8S digital rotational viscometer and spreadability was evaluated by compressing a fixed amount of gel between two glass plates under a standard weight and recording the spreading diameter. Drug-content uniformity was determined by HPLC assay of sinomenine after methanol extraction of the gel. These tests were selected because pH, rheology, drug content and in-use transformation are recognized as critical quality attributes for topical semisolid products (Jin *et al*., 2023).

Experimental animals and ethical statement

Forty-eight New Zealand white rabbits weighing 2.0-2.5 kg were used in this study. The study design included six groups of eight animals each, for a total of 48 animals. All animals were acclimatized for 7 days before model induction under controlled conditions (20-25°C, 45±5% humidity, 12 h light/dark cycle) with free access to food and water. During acclimatization, animals were observed daily for general condition, food intake, body weight, skin integrity and baseline limb activity. All procedures were approved by the Animal Ethics Committee of Guizhou University of Traditional Chinese Medicine (Approval No.: KJ2026-106-02).

Inclusion and exclusion criteria

Animals were included if they were healthy New Zealand white rabbits within the prespecified body-weight range (2.0-2.5 kg), had normal food and water intake, showed no visible skin injury at the application sites and had no signs of infection, lameness, or systemic illness after acclimatization. Animals were excluded before randomization if they had baseline joint swelling, abnormal gait, skin ulceration or dermatitis at ST36 or the non-acupoint site, marked weight loss, severe infection, accidental injury or failure to meet the model-establishment criteria. Animals were also to be excluded during the experiment if humane endpoints were reached, including persistent anorexia, severe distress, weight loss exceeding 20%, uncontrolled infection, severe skin necrosis at the application site or inability to access food or water.

OVA/CFA-induced RA model

OVA and CFA were used in the same animals to induce the RA model according to an established immunization-challenge approach. Briefly, OVA was emulsified with CFA for systemic sensitization, followed by OVA challenge to induce inflammatory joint responses. Model establishment was assessed before intervention using prespecified criteria, including visible periarticular swelling and redness, reduced spontaneous limb use, an arthritis score of at least 2 and an increase in paw volume of at least 30% compared with the pre-modeling baseline. Animals that failed to meet these thresholds or developed unrelated severe illness, infection or application-site skin damage before intervention were excluded according to the criteria described above.

This model was used because antigen-induced arthritis in rabbits can reproduce chronic synovitis and cartilage proteoglycan loss after ovalbumin sensitization and challenge, providing a disease-relevant platform for evaluating anti-inflammatory and joint-protective interventions (Pettipher and Henderson, 1988). The reporting of animal allocation, blinding, inclusion/exclusion criteria and humane endpoints was aligned with ARRIVE 2.0 recommendations for animal research (du Sert *et al*., 2020).

Grouping and interventions

Animals were assigned by simple computer-generated randomization into six groups (n=8 each): normal control group, vehicle-only transdermal control group, acupuncture group, acupoint injection group, ST36-site transdermal Qingteng Waifu San group and adjacent non-acupoint transdermal Qingteng Waifu San group. Random numbers were generated by an investigator who was not involved in intervention delivery or outcome assessment and group assignments were kept in sealed opaque envelopes until allocation. The vehicle-only control group was added to distinguish the pharmacological effect of Qingteng Waifu San from local skin irritation, occlusive dressing and mechanical stimulation caused by transdermal application.

The ST36 region was localized using anatomical landmarks and bone-length proportional methods on the dorsolateral aspect of the hind limb. The adjacent non-acupoint site was selected 2.0 cm lateral to ST36 as a nearby anatomical control.

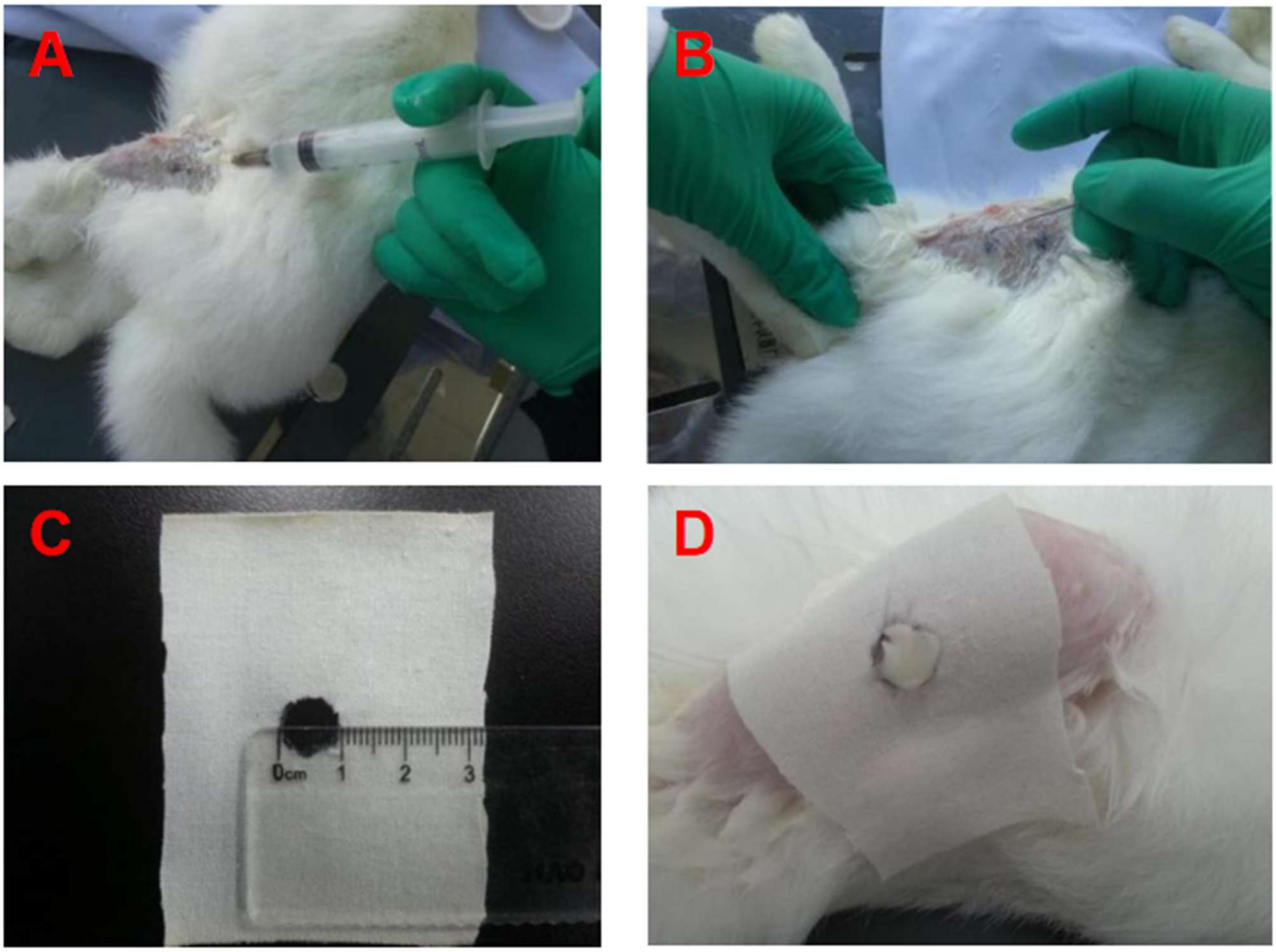

Fig. 1: Intervention and application sites. (A) Acupuncture at ST36; (B) Acupoint injection at ST36; (C) Standardised topical application area; (D) Transdermal application procedure. All panels were replaced or prepared as high-resolution figure files where available.

The normal control group did not undergo RA induction. The vehicle-only transdermal control group underwent the same RA induction procedure and received the same hydrophilic gel base without Qingteng Waifu San at ST36 for 12 h. The ST36 transdermal group received Qingteng Waifu San (QWS) gel at 400 mg/kg for 12 h, applied over a 0.6 cm^2 area. The adjacent non-acupoint group received the same formulation at the corresponding non-acupoint site. The acupuncture group received stimulation with a disposable acupuncture needle at ST36. The acupoint injection group received 2.0 mL of sinomenine solution prepared in water for injection at 400 mg/kg via subcutaneous injection at ST36. The dose was selected according to previous sinomenine acupoint application studies, preliminary tolerability observations and the need to match the topical and injection intervention dose. Figure 1 illustrates the intervention sites and application procedures.

Sample collection and RA efficacy assessment

Blood samples were collected after intervention and centrifuged to obtain serum. Tissue blocks containing skin and underlying subcutaneous tissue were excised from the ST36 and non-acupoint application regions. Tissue samples were rinsed with physiological saline, minced and homogenized using a Mini-Beadbeater-16 tissue homogenizer. Serum and tissue supernatants were stored at -80°C until analysis.

RA-related efficacy was assessed using arthritis score, paw volume, mechanical withdrawal threshold, serum inflammatory cytokines and histopathological scores. Paw volume was measured with a plethysmometer. Mechanical pain sensitivity was assessed using von Frey filaments and the mechanical withdrawal threshold was recorded. Serum TNF-alpha, IL-6 and IL-1beta levels were measured using rabbit-specific ELISA kits. Joint tissues were fixed, decalcified, embedded, sectioned and stained with hematoxylin-eosin and Safranin O/Fast Green. Synovitis, cartilage destruction and bone erosion were scored by two blinded observers.

Table 2: Primer sequences used for real-time PCR.

Primer name	Primer sequence (5′-3′)	Product size (bp)
SP forward	GGAGTCTGTGCTCTGGGATT	143
SP reverse	TGAGGGAGTGAAGGAGCAAC	143
CGRP forward	GAGTACCTGAACCGGCATCT	172
CGRP reverse	GGTATGCACCCAGAGTGATG	172
GAPDH forward	AAGAGGGATGCTGCCCTTAC	119
GAPDH reverse	TACGGCCAAATCCGTTCACA	119

Table 3: Reverse-transcription reaction components.

Reagent	Volume (μL)
5× genomic DNA (gDNA) Eraser buffer	2.0
gDNA Eraser	1.0
Total RNA	5.0
RNase-free water	2.0
Total	10.0

Table 4: Amplification reaction components.

Reagent	Volume (μL)
2× SYBR Premix Ex Taq	12.5
Forward primer	0.5
Reverse primer	0.5
Template cDNA	2.0
Double-distilled water (ddH2O)	4.5

Table 5: Illustrative physicochemical characteristics of Qingteng Waifu San gel and the vehicle-only gel.

Characteristic	Qingteng Waifu San gel	Vehicle-only gel
Appearance	Pale-yellow, translucent, homogeneous; no visible particles or phase separation	Colourless to faintly translucent, homogeneous; no visible particles or phase separation
pH	6.19±0.04	6.16±0.04
Viscosity at 25°C (mPa·s)	18,530±470	18,760±480
Spreadability diameter (cm)	5.68±0.16	5.64±0.17
Sinomenine content (% of nominal content)	99.1±0.9	Not applicable
Content-uniformity RSD (%)	1.23	Not applicable
Principal sinomenine retention time (min)	7.84±0.02	No corresponding peak
HPLC fingerprint similarity	0.990±0.003	Not applicable

Values are presented as mean±SD for a working dataset representing three independently prepared batches with three replicate measurements per batch. RSD, relative standard deviation; HPLC, high-performance liquid chromatography.

Blinding was applied to all outcome assessments whenever technically feasible. Investigators who measured arthritis scores, paw volume, mechanical withdrawal threshold, ELISA and qPCR results and histopathological scores were blinded to group allocation. Histopathological sections were independently scored by two blinded observers and disagreements were resolved by consensus. Statistical analysis was performed after the dataset had been coded and locked.

ELISA, RNA extraction and quantitative real-time PCR (qPCR)

SP, CGRP, TNF-alpha, IL-6 and IL-1beta levels were measured using rabbit-specific ELISA kits according to the manufacturers' instructions. Absorbance was measured at 450 nm using an ELx800 microplate reader (BioTek Instruments, Inc., USA). Standard curves for SP and CGRP are provided in figure S1. Relative messenger RNA (mRNA) expression of SP and CGRP was calculated using the 2^-DeltaDeltaCt method with glyceraldehyde-3-phosphate dehydrogenase (GAPDH) as the internal reference gene and an expected electrophoretic product size was observed (Livak and Schmittgen, 2001).

Total RNA was extracted from tissue samples using RNAiso Plus according to the manufacturer’s protocol.

Table 6: RA disease activity and behavioural pain response after intervention.

Variable	Normal control	Vehicle-only control	QWS-ST36	QWS non-acupoint	Acupuncture	Acupoint injection	Overall P
Arthritis score	0.26±0.15	2.94±0.30	1.63±0.30	2.31±0.32	1.77±0.31	1.41±0.24	<0.001
Paw volume (mL)	1.10±0.09	2.27±0.16	1.83±0.13	1.92±0.26	1.85±0.16	1.54±0.11	<0.001
Mechanical withdrawal threshold (g)	27.16±1.41	9.30±1.66	19.21±2.36	14.79±2.70	16.68±2.29	19.82±2.10	<0.001

Data are presented as mean ±SD, n=8 per group.

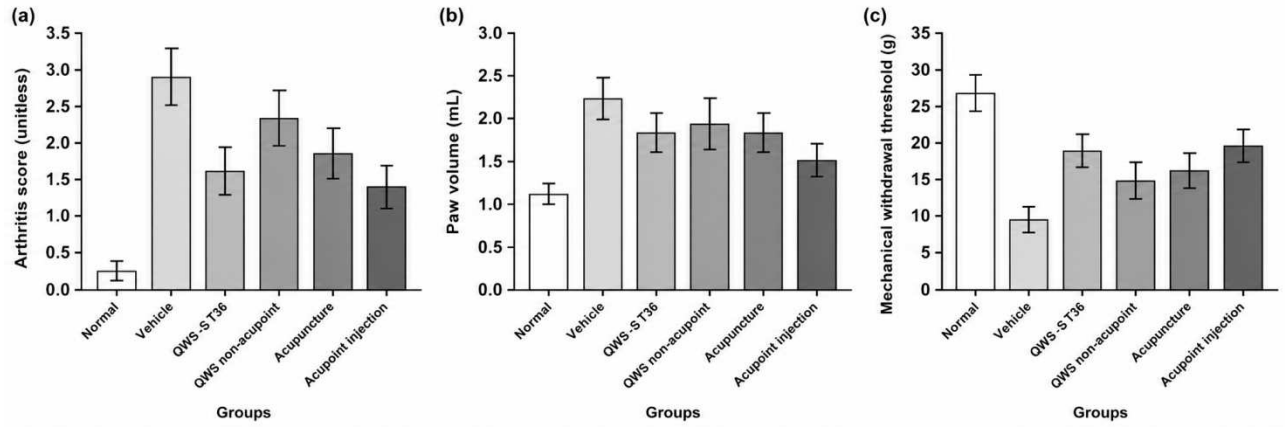

Fig. 2: RA disease activity indicators after intervention. (a) Arthritis score (unitless); (b) Paw volume (mL); (c) Mechanical withdrawal threshold. Data are presented as mean ± SD.

Primer sequences are shown in table 2, reverse transcription components in table 3 and amplification components in Table 4.

Statistical analysis

Data are expressed as mean ± standard deviation (SD). Analyses were performed using SPSS version 26.0 and GraphPad Prism version 10.2. Normality and homogeneity of variance were assessed before group comparisons. One-way analysis of variance (ANOVA) followed by Tukey's post hoc test was used for normally distributed data with homogeneous variance. For ordinal or non-normally distributed variables, the Kruskal-Wallis test followed by Dunn-Bonferroni post hoc comparison was used. A two-sided $P<0.05$ was considered statistically significant. Because animal experiments are particularly vulnerable to bias from allocation and outcome assessment, the statistical workflow was planned together with randomization, blinding and predefined exclusion criteria rather than treated as a separate post hoc procedure (du Sert *et al*., 2020).

RESULTS

Formulation characteristics and quality control

All batches were pale yellow, translucent, and macroscopically homogeneous, with no visible particles, precipitation or phase separation after equilibration. The pooled pH was 6.19±0.04, the viscosity at 25°C was 18,530±470 mPa·s and the spreadability diameter was 5.68±0.16 cm. The vehicle-only gel had comparable pH, viscosity and spreadability, suggesting that incorporation of sinomenine did not materially alter the gross handling characteristics of the Carbomer-based matrix (Table 5). HPLC analysis identified a principal peak corresponding to the sinomenine reference standard at 7.84±0.02 min. The sinomenine content was 99.1±0.9% of the nominal content, the pooled content-uniformity relative standard deviation was 1.23% and fingerprint similarity among the three batches was 0.990±0.003. No corresponding sinomenine peak was detected in the vehicle-only gel.

RA disease activity, pain response and inflammatory cytokines

As shown in Table 6 and Fig. 2, the RA vehicle-only control group showed higher arthritis score and paw volume and a lower mechanical withdrawal threshold than the normal control group. Compared with the vehicle-only control group, ST36-site transdermal Qingteng Waifu San reduced arthritis score and paw volume and increased mechanical withdrawal threshold. The adjacent non-acupoint group showed partial improvement, but the response was generally weaker than that in the ST36-site group.

Table 7: Serum inflammatory cytokine levels after intervention.

Variable	Normal control	Vehicle-only control	QWS-ST36	QWS non-acupoint	Acupuncture	Acupoint injection	Overall P
TNF-alpha (pg/mL)	41.94±4.80	123.40±11.63	78.78±8.82	90.33±6.27	83.49±11.22	64.94±6.49	<0.001
IL-6 (pg/mL)	22.85±2.72	87.97±8.06	58.11±8.57	64.11±10.62	55.17±5.29	45.39±7.44	<0.001
IL-1beta (pg/mL)	28.60±3.40	78.96±10.80	43.40±8.41	57.59±8.51	49.96±3.99	41.08±6.79	<0.001

Data are presented as mean±SD, n=8 per group.

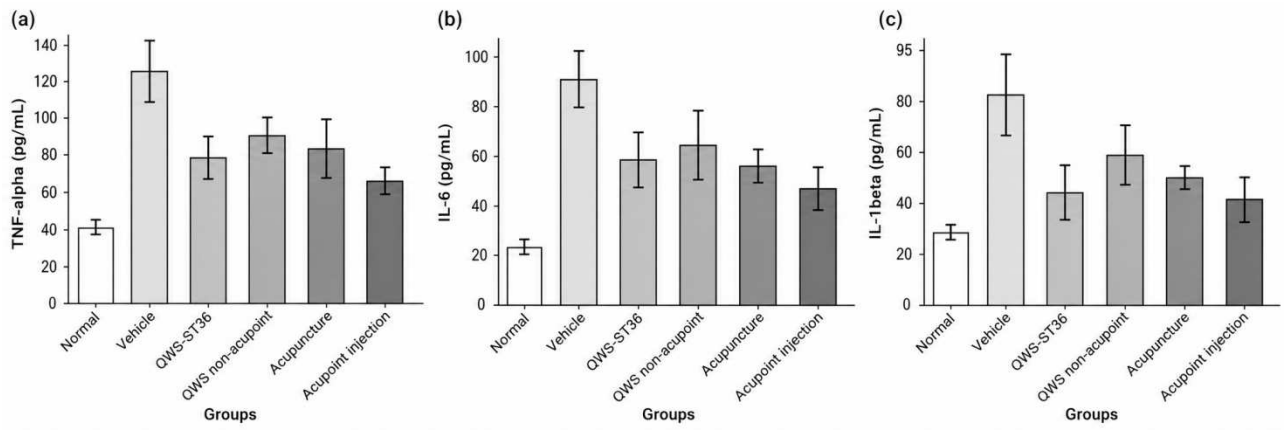

Fig. 3: Serum TNF-alpha, IL-6 and IL-1beta levels after intervention. (a) Serum tumor necrosis factor-alpha (TNF-α) levels (pg/mL); (b) serum interleukin-6 (IL-6) levels (pg/mL); (c) serum interleukin-1 beta (IL-1β) levels (pg/mL). Data are presented as mean ± SD.

Table 8: Histopathological scores of joint tissues.

Variable	Normal control	Vehicle-only control	QWS-ST36	QWS non-acupoint	Acupuncture	Acupoint injection	Overall P
Synovitis score	0.16±0.14	2.85±0.20	1.52±0.20	2.14±0.18	1.71±0.35	1.27±0.18	<0.001
Cartilage destruction score	0.10±0.09	2.50±0.34	1.31±0.17	1.96±0.18	1.69±0.31	1.05±0.32	<0.001
Bone erosion score	0.13±0.13	2.54±0.47	1.10±0.18	1.68±0.27	1.73±0.26	0.93±0.34	<0.001

Data are presented as mean±SD, n=8 per group.

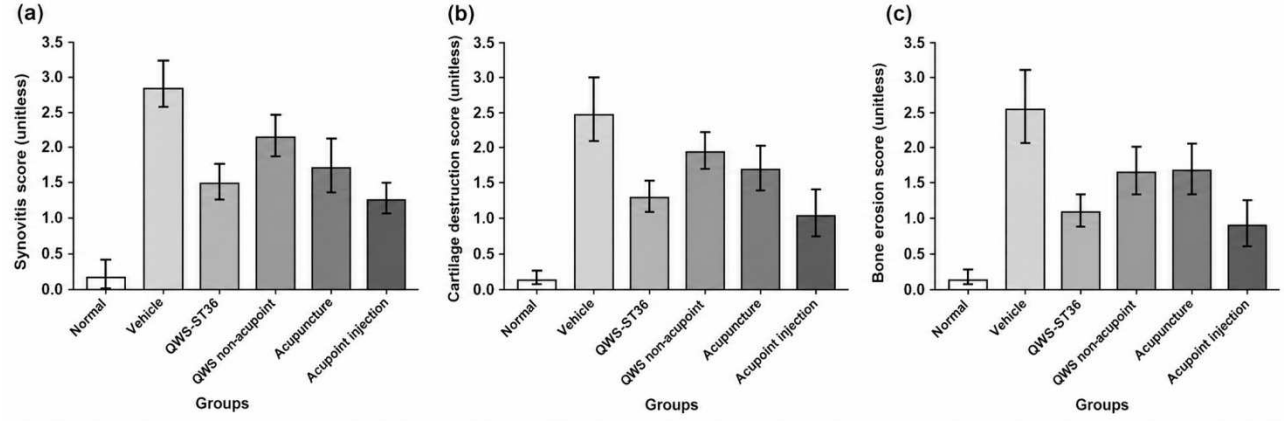

Fig. 4: Histopathological scores: (a) synovitis; (b) cartilage destruction; (c) bone erosion (mean ± SD).

Serum inflammatory cytokine levels are presented in Table 7 and Fig. 3. TNF-alpha, IL-6 and IL-1β were elevated in the vehicle-only control group. ST36-site Qingteng Waifu San reduced all three cytokines compared with vehicle-only control, supporting the addition of disease-relevant inflammatory endpoints.

Table 9: SP content in serum and local tissue.

Group	Blood SP (pg/mL)	Tissue SP (pg/mL)
Normal control	104.52±13.33	87.75±11.46
Vehicle-only control	107.20±12.68	89.84±10.72
QWS-ST36	126.02±14.14	108.42±13.14
QWS non-acupoint	112.50±12.04	92.47±11.25
Acupuncture	154.25±15.47	153.10±17.47
Acupoint injection	179.33±19.59	188.68±20.56

Data are presented as mean±SD, n=8 per group.

Table 10: CGRP content in serum and local tissue.

Group	Blood CGRP (pg/mL)	Tissue CGRP (pg/mL)
Normal control	112.08±13.34	72.69±10.27
Vehicle-only control	113.54±12.92	78.95±9.88
QWS-ST36	158.29±18.31	142.59±16.74
QWS non-acupoint	115.47±13.80	108.24±12.51
Acupuncture	166.26±20.58	154.82±20.63
Acupoint injection	180.51±20.14	195.97±20.35

Data are presented as mean±SD, n=8 per group.

Table 11: Relative expressions of SP mRNA and CGRP mRNA.

Group	SP mRNA (relative expression)	CGRP mRNA (relative expression)
Normal control	0.82±0.09	0.77±0.08
Vehicle-only control	0.83±0.09	0.78±0.08
QWS-ST36	0.90±0.10	0.88±0.10
QWS non-acupoint	0.81±0.09	0.79±0.09
Acupuncture	1.00±0.08	1.00±0.09
Acupoint injection	1.03±0.11	1.02±0.10

Data are presented as mean ±SD, n=8 per group.

Histopathological assessment

Histopathological scores are summarized in Table 8 and Fig. 4. The vehicle-only control group showed increased synovitis, cartilage destruction and bone erosion scores compared with normal controls. These scores were lower in the ST36-site transdermal Qingteng Waifu San group and the acupoint injection group, indicating that inflammatory and structural endpoints should be considered together with SP/CGRP data.

SP and CGRP protein levels

ELISA standard curves used for SP and CGRP quantification are provided in Supplementary Fig. S1. SP concentrations are shown in table 9. SP levels were higher in the ST36 transdermal group than in the adjacent non-acupoint group, but lower than in the acupuncture and acupoint injection groups. Vehicle-only control values were close to the model baseline, supporting the need for this negative transdermal control.

CGRP concentrations are shown in table 10. The ST36 transdermal group had higher CGRP levels than the adjacent non-acupoint group. Because CGRP is involved in neurogenic inflammation and vasodilation, these findings were interpreted as site-dependent neurocutaneous modulation rather than as independent proof of therapeutic benefit.

SP and CGRP mRNA expression

Relative SP and CGRP mRNA levels are shown in Table 11. Consistent with protein-level findings, ST36-site Qingteng Waifu San increased SP and CGRP mRNA expression compared with adjacent non-acupoint application.

DISCUSSION

The present study integrates formulation quality, site-specific transdermal delivery, neuropeptide signaling and disease-relevant RA outcomes in a rabbit antigen-induced arthritis model. The principal finding was not simply that ST36-site application altered SP and CGRP, but that this neurocutaneous response occurred alongside lower arthritis activity, reduced paw swelling,

improved mechanical withdrawal threshold, lower circulating TNF-alpha, IL-6 and IL-1beta and less severe synovitis, cartilage destruction and bone erosion. The adjacent non-acupoint group showed a weaker overall response, whereas acupoint injection generally produced the largest numerical improvement. Taken together, the data support a model in which both the pharmacological action of sinomenine and the biological properties of the site of application contribute to the observed response; they do not establish that elevation of neuropeptides themselves is anti-arthritic.

The formulation-characterization section provides essential pharmaceutical context for the biological findings. The narrow variation in pH (6.19±0.04), viscosity (18,530±470 mPa·s), spreadability (5.68±0.16 cm), sinomenine content (99.1±0.9% of the label claim) and HPLC fingerprint similarity (0.990±0.003) indicates reproducible preparation of the Carbomer-based semisolid across three batches. This finding is important because the performance of a topical product depends not only on the pharmacological activity of sinomenine but also on the behaviour of the vehicle during application. Evaporation, shear, hydration and rheological metamorphosis may alter the thermodynamic activity of drugs and skin permeation under in-use conditions (Jin *et al*., 2022; Jin *et al*., 2023). Various delivery strategies have also been developed to address the limited bioavailability and formulation constraints of sinomenine (Chen *et al*., 2022), while robust chemical quality control remains essential for products derived from Sinomenium acutum (Huang *et al*., 2020). Compared with sinomenine-loaded antioxidant transethosomes, which have been reported to enhance skin permeation and local drug deposition, the present Carbomer gel is simpler and non-invasive but relies more heavily on passive diffusion, occlusion and residence time.

The vehicle-only group developed the expected phenotype of antigen-induced arthritis, including marked increases in arthritis score and paw volume, mechanical hypersensitivity, elevated inflammatory cytokines and histological joint injury. This pattern is consistent with the classic rabbit ovalbumin arthritis model, in which antigen challenge produces persistent synovitis and cartilage proteoglycan loss and with more recent experimental work showing that antigen-induced arthritis provides relatively stable swelling, pain and inflammatory-pathway readouts (Pettipher and Henderson, 1988; Zhang *et al*., 2023). The concurrent deterioration in behavioural, biochemical and structural outcomes strengthens confidence that the model represented active inflammatory arthritis rather than isolated edema or nociception.

Relative to the vehicle-only group, the ST36 transdermal group showed an approximately 44.6% lower arthritis score and 19.4% lower paw volume, while the mechanical withdrawal threshold was approximately doubled. These changes are directionally consistent with the 2026 meta-analysis of 38 sinomenine animal studies, which found pooled reductions in arthritis index and paw volume, although substantial heterogeneity was attributed to dose, duration and administration route (Li *et al*., 2026). They also parallel studies of ST36 acupuncture in adjuvant- or antigen-induced arthritis, where treatment reduced joint swelling and improved nociceptive thresholds (Yang *et al*., 2021). The present work extends that literature by showing that a non-invasive drug-containing gel applied at ST36 can generate a response profile intermediate between adjacent non-acupoint application and direct acupoint injection. Nevertheless, mechanical withdrawal threshold should not be treated as a surrogate for inflammation alone, because RA pain can persist through neuronal sensitization, autoantibody-neuron interactions and fibroblast-neuron signaling even when synovitis is partly controlled (Cao *et al*., 2020; Rutter-Locher *et al*., 2024).

The cytokine findings provide a pharmacologically coherent link between clinical disease activity and tissue injury. Compared with the vehicle-only control, the ST36 group showed descriptive reductions of approximately 36.2% in TNF-α, 33.9% in IL-6 and 45.0% in IL-1β. This pattern is consistent with previous evidence showing that sinomenine can inhibit experimental RA progression by modulating inflammatory cytokine secretion and monocyte/macrophage subsets, as well as with more recent findings suggesting suppression of phosphoinositide 3-kinase/protein kinase B (PI3K–Akt)-related immune activation (Liu et al., 2024; Iadecola et al., 2017). It also aligns with a recent preclinical meta-analysis reporting reductions in TNF-α, IL-1β, and IL-6 across sinomenine-treated RA models, although substantial heterogeneity was observed (Li et al., 2026). Additional mechanistic studies have linked improved arthritis outcomes to regulation of neutrophil-associated nuclear factor kappa B/mitogen-activated protein kinase (NF-κB/MAPK) activity and to IL-6 promoter methylation. However, these pathways were not directly examined in the present study. Therefore, the observed cytokine

reductions should be interpreted as convergent evidence of anti-inflammatory activity rather than as proof of a single molecular mechanism.

Histopathology supported the biochemical findings. Synovitis, cartilage destruction and bone erosion scores in the ST36 group were descriptively 46.7%, 47.6% and 56.7% lower, respectively, than in the vehicle-only group. This concordance is important because improvement in serum cytokines without preservation of joint structure would offer limited evidence of disease modification. The direction of the present findings agrees with the joint-protective component of the sinomenine animal meta-analysis and with local biomaterial studies that combine sinomenine delivery with immune regulation and bone repair (Cai *et al*., 2026). The acupoint injection group showed the lowest histopathological scores, consistent with the route-dependent effects reported in the meta-analysis, in which injectable administration produced relatively robust efficacy. However, direct injection alters both tissue exposure and the mechanical stimulus; therefore, it cannot be used to attribute the response exclusively to acupoint biology.

The comparison with acupuncture further clarifies the interpretation of ST36 specificity. Experimental studies have shown that ST36 stimulation can regulate macrophage communication, reduce TNF-alpha and IL-1beta, promote tissue-repair programs and engage local sensory transduction pathways. Further evidence indicates that transient receptor potential ankyrin 1 (TRPA1) at ST36 contributes to acupuncture-induced analgesia in arthritic mice, supporting the view that this acupoint functions as a biologically responsive neuroimmune interface rather than merely as a geometric location (Yao *et al*., 2024; Luo *et al*., 2026). In the present study, the transdermal ST36 group generally performed better than the adjacent non-acupoint group but not uniformly better than acupuncture or injection. This graded pattern is biologically plausible: topical application combines passive drug delivery, occlusion and cutaneous stimulation; acupuncture adds a stronger mechanical afferent signal; and injection provides direct local exposure plus needle stimulation (Livak KJ and Schmittgen TD., 2001).

SP and CGRP require particularly careful discussion. The ST36 gel group had higher SP and CGRP protein concentrations than the adjacent non-acupoint group in both serum and local tissue; the corresponding differences were approximately 12.0% and 17.2% for SP and 37.1% and 31.7% for CGRP. SP and CGRP mRNA were also about 11% higher at ST36. These results support site-dependent neurocutaneous activation, but neither peptide is intrinsically beneficial in RA. SP can facilitate vasodilation, plasma extravasation, mast cell activation, and nociceptive transmission, while CGRP has context-dependent vascular, sensory, and immunomodulatory effects in joints (Matsuda *et al*., 2019; Liu *et al*., 2018). Contemporary models of cutaneous neurogenic inflammation similarly place TRP channels, SP, CGRP, mast cells, endothelium and immune cells within a bidirectional network (Marek-Jozefowicz *et al*., 2023). Thus, the most defensible interpretation is that the application of ST36 elicited a stronger local afferent-neurovascular response, while the simultaneous reduction in cytokines and structural injury indicates that this response occurred within an overall anti-inflammatory treatment context. Causality between neuropeptide elevation and improvement in arthritis was not established.

The partial response observed at the adjacent non-acupoint site is also informative. It suggests that sinomenine exerted a pharmacological effect independent of precise acupoint placement, whereas the stronger response at ST36 may reflect regional differences in sensory-nerve distribution, microvascular perfusion, skin thickness, appendage density, or local immune-cell composition. Microdialysis combined with ultra-performance liquid chromatography-tandem mass spectrometry (UPLC–MS/MS) has demonstrated the relevance of local sinomenine exposure during acupoint application (Wang *et al*., 2019; Choi *et al*., 2018). However, site specificity appears to vary across delivery platforms. Triptolide-loaded dissolving microneedles have been shown to reduce inflammation, joint swelling, and bone erosion, with no significant difference between acupoint and non-acupoint administration (Li *et al*., 2024; Jiang *et al*., 2025). This contrast is important because microneedles bypass the stratum corneum and may therefore minimize regional differences in passive permeability, whereas the present gel relies on hydration, diffusion, occlusion and local skin physiology. Differences in the active compound, animal model, control-site selection and treatment schedule may also have contributed. Because the present study did not measure local sinomenine concentration, skin blood flow, or nerve-fiber density, the mechanism underlying the stronger ST36 response remains uncertain. In addition, the non-acupoint site was located only 2 cm from ST36, so regional neurovascular overlap may have attenuated or distorted the apparent site-specific contrast.

Several strengths distinguish this study from earlier acupoint-application reports: inclusion of a vehicle-only transdermal control, direct comparison with an adjacent non-acupoint site, simultaneous assessment of pain, inflammation and joint structure, blinded outcome assessment and parallel measurement of SP/CGRP at the protein and transcript levels. Important limitations remain. The sample size was modest and no a priori power calculation was reported. Only one dose and one exposure duration were tested. Pairwise post hoc estimates and confidence intervals should be reported rather than relying only on overall P values. SP/CGRP receptor blockade or sensory-denervation experiments would be needed to establish mechanistic necessity. Finally, the rabbit antigen-induced model captures selected inflammatory and structural features of RA but cannot reproduce the full chronic, systemic and heterogeneous nature of human disease.

CONCLUSION

Subject to verification of the formulation-characterization data, Qingteng Waifu San gel applied at ST36 produced a stronger SP/CGRP neurocutaneous response than adjacent non-acupoint application and was accompanied by more favourable inflammatory, behavioural and histopathological profiles than vehicle-only control in this rabbit model. The findings support further pharmaceutical, pharmacokinetic and mechanistic evaluation of site-specific transdermal sinomenine delivery, but they do not establish that neuropeptide elevation mediates benefit or that the formulation is ready for clinical use.

Acknowledgments
The authors gratefully acknowledge financial support from the National Natural Science Foundation of China and the National Miao Medicine Engineering Technology Research Center.

Authors' contributions
Yuan Gao and Lei Chi: Contributed to study design and manuscript drafting; Kun Gao and Yanning Liu: Performed animal experiments and data acquisition; Mengdan Zhou: Supervised the project and revised the manuscript. All authors approved the final version.

Funding
This study was supported by the National Natural Science Foundation of China Regional Science Foundation Project (No. 82260885) and the Capacity Enhancement Project for the National Miao Medicine Engineering Technology Research Center (Qiankehe Zhong Yin Di [2023] No. 006).

Data availability statement
The datasets generated during and/or analysed during the current study are available from the corresponding author on reasonable request.

Ethical approval
All animal procedures were approved by the Animal Ethics Committee of Guizhou University of Traditional Chinese Medicine (Approval No. KJ2026-106-02). This study was performed in adherence with the ARRIVE guidelines. See supplementary file for the ARRIVE checklist.

Conflict of interest
The authors declare no conflict of interest.

Supplementary data
https://pjps.pk/uploads/2026/08/SUP1787837141.pdf

REFERENCES

Cai L, Gao J, Zhang K, Xiao B, Xu S, Zhao W, Li J, Zhou Y, Zhu W, Liu S, Pei T, Li J, Chen Y, Chen S, Li J and Li J (2026). Hydrogel microspheres loaded with sinomenine and Drynaria rhizome enhance the treatment of rheumatoid arthritis via immune regulation and promoting bone repair. *J. Nanobiotechnol.*, **24**(1): 174.

Cao Y, Fan D and Yin Y (2020). Pain mechanism in rheumatoid arthritis: From cytokines to central sensitization. *Mediators Inflamm.*, **2020**: 2076328.

Chen X, Li C, Cao X, Tu T, Tang N, Xu L and Liu L (2022). Recent advancements in drug delivery of sinomenine, a disease-modifying anti-rheumatic drug. *Pharmaceutics*, **14**(12): 2820.

Choi JE and Di Nardo A (2018). Skin neurogenic inflammation. *Semin. Immunopathol.*, **40**(3): 249-259.

du Sert NP, Hurst V, Ahluwalia A, Alam S, Avey MT, Baker M, Browne WJ, Clark A, Cuthill IC, Dirnagl U, Emerson M, Garner P, Holgate ST, Howells DW, Karp NA, Lazic SE, Lidster K, MacCallum CJ, Macleod M, Pearl EJ, Petersen OH, Rawle F, Reynolds P, Rooney K, Sena ES, Silberberg SD, Steckler T and Würbel H (2020). The ARRIVE guidelines 2.0: Updated guidelines for reporting animal research. *PLoS Biol.*, **18**(7): e3000410.

Green PG (2005). Gastrin-releasing peptide, substance P and cytokines in rheumatoid arthritis. *Arthritis Res. Ther.*, **7**(3): 111-113.

Huang YF, He F, Wang CJ, Xie Y, Zhang YY, Sang Z, Qiu P, Luo P, Xiao SY, Li J, Wu FC, Liu L and Zhou H (2020). Discovery of chemical markers for improving the quality and safety control of

sinomenium acutum stem by the simultaneous determination of multiple alkaloids using UHPLC-QQQ-MS/MS. *Sci. Rep.*, **10**(1): 14182.

Iadecola C (2017). The neurovascular unit coming of age: A journey through neurovascular coupling in health and disease. *Neuron*, **96**(1): 17-42.

Jiang H, Lu Q, Huang X, Zhang H, Zeng J, Wang M, Xu J, Yuan Z, Wei Q and Xiao E (2025). sinomenine-glycyrrhizic acid self-assembly enhanced the anti-inflammatory effect of sinomenine in the treatment of rheumatoid arthritis. *J. Control Release*, **382**: 113718.

Jin X, Alavi SE, Shafiee A, Leite-Silva VR, Khosrotehrani K and Mohammed Y (2023). Metamorphosis of topical semisolid products-understanding the role of rheological properties in drug permeation under the "in use" condition. *Pharmaceutics*, **15**(6): 1707.

Jin X, Imran M and Mohammed Y (2022). Topical semisolid products-understanding the impact of metamorphosis on skin penetration and physicochemical properties. *Pharmaceutics*, **14**(11): 2487.

Li G, Zheng YC, He R and Gao JL (2026). Sinomenine ameliorates rheumatoid arthritis in rodent models: A systematic review and meta-analysis of anti-inflammatory and joint-protective effects. *Front. Pharmacol.*, **17**: 1800265.

Li S, Chen Q, Zhang Y, Wang D, Hu H, Li J, Zhang C and Zhang J (2024). Hyaluronic acid dissolving microneedle patch-assisted acupoint transdermal delivery of triptolide for effective rheumatoid arthritis treatment. *Sci. Rep.*, **14**(1): 25256.

Lisowska B, Kosson D and Domaracka K (2015). Substance P and chronic pain in patients with chronic inflammation of connective tissue. *PLoS One*, **10**(10): e0139206.

Liu Q, Wang J, Ding C, Chu Y, Jiang F, Hu Y, Li H and Wang Q (2024). Sinomenine alleviates rheumatoid arthritis by suppressing the PI3K-Akt signaling pathway, as demonstrated through network pharmacology, molecular docking and experimental validation. *Drug Des. Devel. Ther.*, **18**: 3523-3545.

Liu W, Zhang Y, Zhu W, Ma C, Ruan J, Long H, Wang Y, Li W and Wang Y (2018). Sinomenine inhibits the progression of rheumatoid arthritis by regulating the secretion of inflammatory cytokines and monocyte/macrophage subsets. *Front. Immunol.*, **9**: 2228.

Livak KJ and Schmittgen TD (2001). Analysis of relative gene expression data using real-time quantitative PCR and the 2(-Delta Delta C(T)) method. *Methods*, **25**(4): 402-408.

Luo JF, Yu Y, Yao YD, Zhang C, Liu JX, Lio C, Qian HB and Zhou H (2026). Sinomenine treats rheumatoid arthritis by regulating IL-6 gene promoter methylation. *Phytomedicine*, **153**: 157793.

Marek-Jozefowicz L, Nedoszytko B, Grochocka M, Zmijewski MA, Czajkowski R, Cubala WJ and Slominski AT (2023). Molecular mechanisms of neurogenic inflammation of the skin. *Int. J. Mol. Sci.*, **24**(5): 5001.

Matsuda M, Huh Y and Ji RR (2019). Roles of inflammation, neurogenic inflammation and neuroinflammation in pain. *J. Anesth.*, **33**(1): 131-139.

Pettipher ER and Henderson B (1988). The relationship between cell-mediated immunity and cartilage degradation in antigen-induced arthritis in the rabbit. *Br. J. Exp. Pathol.*, **69**(1): 113-122.

Rutter-Locher Z, Kirkham BW, Bannister K, Bennett DL, Buckley CD, Taams LS and Denk F (2024). An interdisciplinary perspective on peripheral drivers of pain in rheumatoid arthritis. *Nat. Rev. Rheumatol.*, **20**(11): 671-682.

Song H, Wen J, Li H, Meng Y, Zhang Y, Zhang N and Zheng W (2019). Enhanced transdermal permeability and drug deposition of rheumatoid arthritis via sinomenine hydrochloride-loaded antioxidant surface transethosome. *Int. J. Nanomedicine*, **14**: 3177-3188.

Walsh DA, McWilliams DF and Mapp PI (2015). Calcitonin gene-related peptide in the joint. *Front. Neurosci.*, **9**: 257.

Wang R, Yang J, Liu Y, Guan B, Feng Q, Wang Y, Lv S, Yang Z and Li Y (2019). The effect of acupoint application of sinomenine for rheumatoid arthritis measured by microdialysis and UPLC-MS/MS. *Evid. Based Complement. Alternat. Med.*, **2019**: 5135692.

Wang W, Wang Z, Ling A, Zhang C, Lv M, Huang L and Niu Y (2025). Research progress in treatment of rheumatoid arthritis with sinomenine and related formulations based on different administration routes. *Front. Pharmacol.*, **16**: 1613679.

Xu Y, Zhao M, Cao J, Fang T, Zhang J, Zhen Y, Wu F, Yu X, Liu Y, Li J and Wang D (2023). Applications and recent advances in transdermal drug delivery systems for the treatment of rheumatoid arthritis. *Acta Pharm. Sin. B*, **13**(11): 4417-4441.

Yang F, Gong Y, Yu N, Yao L, Zhao X, Hong S, Wang S, Chen B, Xu Y, Pang G, Wang H, Guo Y, Li Y, Guo Y and Xu Z (2021). ST36 acupuncture alleviates the inflammation of adjuvant-induced arthritic rats by targeting monocyte/macrophage modulation. *Evid. Based Complement. Alternat. Med.*, **2021**: 9430501.

Yao K, Chen Z, Li Y, Dou B, Xu Z, Ma Y, Du S, Wang J, Fu J, Liu Q, Fan Z, Liu Y, Lin X, Xu Y,

Fang Y, Wang S and Guo Y (2024). TRPA1 ion channel mediates the analgesic effects of acupuncture at the ST36 acupoint in mice suffering from arthritis. *J. Inflamm. Res.*, **17**: 1823-1837.

Zhang C, Zhang S, Liao J, Gong Z, Chai X and Lyu H (2022). Towards better sinomenine-type drugs to treat rheumatoid arthritis: Molecular mechanisms and structural modification. *Molecules*, **27**(24): 8645.

Zhang Y, Wang H, Gong YN, Yang FM, Wang SJ, Liu YY, Gui YQ, Xie F, Xu ZF and Guo Y (2023). Pathological pathway analysis in an experimental rheumatoid arthritis model and the tissue repair effect of acupuncture at ST36. *Front. Immunol.*, **14**: 1164157.